

Reexamining Black–Body Shifts for Hydrogenlike Ions

Ulrich D. Jentschura^{1,2} and Martin Haas³

¹*Max-Planck-Institut für Kernphysik, Postfach 10 39 80, 69029 Heidelberg, Germany*

²*Institut für Theoretische Physik, Philosophenweg 16, 69120 Heidelberg, Germany*

³*Department of Diagnostic Radiology, Medical Physics,
University Hospital Freiburg, 79095 Freiburg, Germany*

We investigate black-body induced energy shifts for low-lying levels of atomic systems, with a special emphasis on transitions used in current and planned high-precision experiments on atomic hydrogen and ionized helium. Fine-structure and Lamb-shift induced black-body shifts are found to increase with the square of the nuclear charge number, whereas black-body shifts due to virtual transitions decrease with increasing nuclear charge as the fourth power of the nuclear charge. We also investigate the decay width acquired by the ground state of atomic hydrogen, due to interaction with black-body photons. The corresponding width is due to an instability against excitation to higher excited atomic levels, and due to black-body induced ionization. These effects limit the lifetime of even the most fundamental, a priori absolutely stable, “asymptotic” state of atomic theory, namely the ground state of atomic hydrogen.

PACS numbers: 12.20.Ds, 31.15.-p, 42.50.Hz

I. INTRODUCTION

Energy shifts of atomic levels due to interactions with black-body radiation are primarily important for Rydberg states, where large dipole polarizabilities enhance the magnitude of the effect [1, 2, 3], but at the current rate of advance of high-precision spectroscopy, its importance for the correct realization of frequency standards has also been stressed in the literature [4, 5, 6, 7]. In particular, the work of Farley and Wing [2] was mainly focused on Rydberg states, which were accessible to high-precision spectroscopy at the time. In contrast, we here focus on the ground state and on the $2S$ state of hydrogen and hydrogenlike ions. The transition frequencies in these systems have only recently come within reach of high-precision laser spectroscopy, due to the development of frequency combs. In all cases studied by Farley and Wing [2], the Lamb shift and fine structure shifts could be neglected, but this does not hold for the transitions studied here.

Ionization by black-body radiation also is an important effect for excited atomic states. The ionization process leads to a finite width of the states (resonances), with the energy acquiring a (small) imaginary part. The sign of the imaginary part is negative, and we can write the black-body induced energy shift $\Delta\mathcal{E}_{\text{bb}}$ as

$$\Delta\mathcal{E}_{\text{bb}} = \Delta E_{\text{bb}} - i \frac{\Delta\Gamma_{\text{bb}}}{2} \quad (1)$$

where ΔE_{bb} is the real part of the energy shift, and $\Delta\Gamma_{\text{bb}}/h$ is the black-body induced width.

Several peculiarities characterize the black-body induced radiative shift. First of all, we recall that two virtual processes contribute: one where the atom absorbs a black-body photon and then returns to the reference state by emission into the same mode of the electromagnetic field from which a photon had been absorbed, and another one where the sequence of absorption and emis-

sion processes is reversed. This is very much analogous to the so-called ac Stark shift (see, e.g., [8, 9]) that an atom feels in a laser field, but with the difference that the black-body radiation is isotropic, and that the polarization vectors are equally distributed among all possible directions in space. For the ground state being the reference state, the “width” (imaginary part of the energy shift) is exclusively generated by the absorption-first channel, where one of the propagator denominators becomes resonant and the virtual state takes the role of the final state of the ionization or excitation process [10]. Note that recently [11], a finite width has been predicted for the ground state of hydrogen at very high temperatures on the basis of field-theoretical considerations [see Eq. (23) of Ref. [11]].

One observation, potentially of fundamental interest, substantiated here by a concrete calculation, is that even the $1S$ state of atomic hydrogen, acquires a finite width when the hydrogen atom is exposed to black-body radiation, although the ground state of the most fundamental atomic system is otherwise assumed to be the perfect “asymptotic state” used in all S -matrix type calculations regarding the quantum electrodynamic (QED) shifts of energy levels [12, 13, 14]. However, before we come to an analysis of this effect, we briefly revisit the evaluation of the real part of the black-body induced energy shifts, for the $1S$ – $2S$ transition in hydrogen [15, 16] and ionized helium (see Sec. II). We then analyze the imaginary parts of the black-body induced energy shifts in Sec. III. Conclusions are drawn in Sec. IV.

II. REAL PARTS OF BLACK-BODY RADIATION INDUCED ENERGY SHIFTS

For clarity, we keep all factors of h , c and ϵ_0 in all calculations. The Boltzmann constant is denoted k_B . We recall that the energy distribution per frequency interval

$d\nu$ of black-body radiation is

$$\rho(\nu) d\nu = \frac{8\pi h \nu^3}{c^3} \left[\exp\left(\frac{h\nu}{k_B T}\right) - 1 \right]^{-1} d\nu, \quad (2)$$

which is connected to the time-averaged square of the electric field $\bar{e}^2(\nu)$ at frequency ν (in units of the square of the electric field strength per frequency) as

$$\bar{e}^2(\nu) d\nu = \frac{1}{\epsilon_0} \rho(\nu) d\nu. \quad (3)$$

We write the Cartesian coordinates as x^i and rewrite the dipole polarizability of an nS state to take the isotropic character of the polarization vectors of black-body radiation into account [cf. Eq. (20) of Ref. [9]]. Then, the black-body energy shift $\Delta E_{\text{bb}}(nS)$ is given by the formulas

$$P_\nu(nS) = \sum_{\pm} \sum_{i=1}^3 \frac{1}{3} \left\langle nS \left| x^i \frac{1}{H - E(nS) \pm h\nu} x^i \right| nS \right\rangle, \quad (4a)$$

$$\Delta E_{\text{bb}}(nS) = -\frac{e^2}{2} (\text{P.V.}) \int_0^\infty d\nu \bar{e}^2(\nu) P_\nu(nS), \quad (4b)$$

where $E(nS)$ is the energy of the reference nS state. The latter integral actually has to be taken as a principal-value (P.V.) integral because the propagator denominators in (4a) can become singular when a black-body photon hits an atomic resonance (see the discussion below in Sec. III).

For the $1S$ state, the properties of the dipole polarizability $P_\nu(1S)$ are well understood [17], and $P_\nu(1S)$ can be evaluated using an entirely nonrelativistic approximation [18], and H in (4a) may be replaced by the Schrödinger Hamiltonian. To see why that is the case, let us consider the typical photon frequencies at which the black-body photon energy peaks. Ignoring the “−1” in the denominator of (3), it is easy to derive the result

$$\nu_{\text{max}} \approx \frac{3k_B T}{h} \quad (5)$$

for the frequency at which $\rho(\nu)$ assumes its maximum value. We consider a temperature range from 4 K...300 K. In this temperature range, the frequency ν_{max} varies from 2.5×10^{11} Hz to 1.9×10^{13} Hz, which is well below the Rydberg constant expressed in frequency units, $R_\infty c = 3.298 \times 10^{15}$ Hz, which defines the frequency range for the virtual excitations to P levels that are decisive for the evaluation of the dipole polarizability. For the ground state acting as the reference state, we may therefore even ignore the terms $\pm h\nu$ in the propagator denominators in (4a) and replace the dynamic by the static polarizability, which can be evaluated easily and is used here in the nonrelativistic approximation (cf. Ref. [19])

$$P_0(1S) = \frac{9}{2} \left(\frac{\hbar}{m_e c} \right)^2 \frac{1}{(Z\alpha)^4 m_e c^2}. \quad (6)$$

TABLE I: Black-body energy shift of the ground state of atomic hydrogen and ionized atomic helium, at a temperature of $T = 4$ K, $T = 77$ K and $T = 300$ K. The shift $\Delta E_{\text{bb}}(1S)$ is obtained by numerical integration according to Eq. (4b) and divided by the Planck constant in order to be expressed in frequency units.

Nucl. charge number	Temperature	$h^{-1} \Delta E_{\text{bb}}(1S)$
$Z = 1$	4 K	-1.22×10^{-9} Hz
$Z = 1$	77 K	-1.68×10^{-4} Hz
$Z = 1$	300 K	-3.88×10^{-2} Hz
$Z = 2$	4 K	-7.65×10^{-12} Hz
$Z = 2$	77 K	-1.05×10^{-5} Hz
$Z = 2$	300 K	-2.42×10^{-3} Hz

The dipole polarizability defined in Eq. (4a) parametrically scales as Z^{-4} , because the energy differences in the propagator denominators scale with Z^2 , whereas the two dipole transition matrix elements in the numerator each acquire a factor $1/Z$ (the atom becomes “smaller” by a factor Z^{-1} as the nuclear charge number increases). We finally obtain the approximation

$$\Delta E_{\text{bb}}(1S) \approx -\frac{3\pi^3 k_B^4}{5 \alpha^3 m_e^3 c^6} \frac{T^4}{Z^4}. \quad (7)$$

The corresponding data in Table I are in excellent agreement with this approximation.

A subtle point concerns the dipole polarizability of excited states [19]: While for the $1S$ state, it is entirely sufficient to approximate H by the Schrödinger Hamiltonian, this is not the case for the $2S$ state and for higher excited nS states with $n > 2$. Indeed, the $2P_{1/2}$ state is displaced from $2S$ only by the Lamb shift, and the $2P_{3/2}$ state is displaced in energy only by the fine-structure, and yet, the dipole transition matrix elements between the $2S$ and the $2P$ states are manifestly nonvanishing. The dipole transition matrix elements which enter the numerators for the dipole polarizability, can still be taken in a non-relativistic approximation, but the denominators must be adjusted for the Lamb shift and the fine-structure effects.

In summary, we have for an nS level with $n \geq 2$,

$$\begin{aligned}
P_\nu(nS) &= \frac{1}{3} \sum_{\pm} \sum_{i=1}^3 \sum_{\mu=-1/2}^{1/2} \frac{|\langle nS_{1/2}(m=\frac{1}{2}) | x^i | nP_{1/2}(m=\mu) \rangle|^2}{E(nP_{1/2}) - E(nS) \pm h\nu} \\
&+ \frac{1}{3} \sum_{\pm} \sum_{i=1}^3 \sum_{\mu=-3/2}^{3/2} \frac{|\langle nS_{1/2}(m=\frac{1}{2}) | x^i | nP_{3/2}(m=\mu) \rangle|^2}{E(nP_{3/2}) - E(nS) \pm h\nu} \\
&+ \frac{1}{3} \sum_{\pm} \sum_{i=1}^3 \sum_{\mu=-1}^1 \sum_{n' \neq n} \frac{|\langle nS(m=0) | x^i | n'P(m=\mu) \rangle|^2}{E(n'P) - E(nS) \pm h\nu}.
\end{aligned} \tag{8}$$

Here, the $|nS_{1/2}\rangle$, the $|nP_{1/2}\rangle$ and the $|nP_{3/2}\rangle$ states can be approximated by Schrödinger–Pauli wave functions, i.e. the radial part is taken in the nonrelativistic approximation, but the angular part is given by a spinor (two-component) function $\chi_\mu^\kappa(\hat{r})$ defined as in [20]; $\kappa = 2(l-j)$ ($j+1/2$) is the Dirac angular quantum number, with l being the orbital angular momentum quantum number and j the total electron angular momentum, and $\mu \in \{-(j+1/2), \dots, j+1/2\}$ is the magnetic projection (half-integer). The states nP and $2S$, by contrast, are plain nonrelativistic Schrödinger eigenstates with an angular part of the form $Y_{lm}(\hat{r})$, where l is the orbital angular momentum, and $m \in \{-l, \dots, l\}$ is the magnetic projection (integer).

In the following, we concentrate on the case $n = 2$, i.e. on the black-body shift of the $2S$ state. The key to finding an analytic approximation to $\Delta E_{\text{bb}}(2S)$ is the following. We observe that for most cases of interest studied here, the condition

$$E_{\text{fs}} \ll h\nu_{\text{max}} \ll hR_\infty c, \tag{9}$$

is fulfilled, where $R_\infty c \approx 3.289 \times 10^{15}$ Hz is the Rydberg constant expressed in frequency units. This hierarchy means that we can make different approximations for the first two as opposed to the third term on the right-hand side of (8). Namely, the relevant frequency range of the black-body radiation is large as compared to the fine-structure and the Lamb shift, but small in comparison to the frequencies corresponding to transition with a change in the principal quantum number. For the last term, of (8), we can thus make the static approximation and obtain

$$\begin{aligned}
P'_0(2S) &= \lim_{\nu \rightarrow 0} \sum_{\pm} \sum_{i=1}^3 \sum_{\mu=-1}^1 \sum_{n'=3}^{\infty} \\
&\times \frac{1}{3} \frac{|\langle 2S(m=0) | x^i | n'P(m=\mu) \rangle|^2}{E(n'P) - E(2S) \pm h\nu} \\
&= 120 \left(\frac{\hbar}{m_e c} \right)^2 \frac{1}{(Z\alpha)^4 m_e c^2},
\end{aligned} \tag{10}$$

where we reemphasize that the sum over n' starts from $n' = 3$. The corresponding energy shift is

$$\Delta E'_{\text{bb}}(2S) \approx -\frac{16\pi^3 k_B^4}{\alpha^3 m_e^3 c^6} \frac{T^4}{Z^4}. \tag{11}$$

For the black-body shift corresponding to the first two terms on the right-hand side of (8), we first recall the fine-structure interval and the Lamb shift in leading order,

$$E_{\text{fs}} = E(2P_{3/2}) - E(2S_{1/2}) = \frac{(Z\alpha)^4 m_e c^2}{32}, \tag{12a}$$

$$E_{\text{L}} = E(2S_{1/2}) - E(2P_{1/2}) = \frac{\alpha}{8\pi} (Z\alpha)^4 m_e c^2 \tag{12b}$$

$$\times \left\{ \frac{4}{3} \ln [(Z\alpha)^{-2}] + \frac{4}{3} (\ln k_0(2P) - \ln k_0(2S)) + \frac{91}{90} \right\}.$$

Here, we make the opposite approximation and expand the terms for large ν ,

$$\begin{aligned}
P''_\nu(2S) &= \frac{1}{3} \sum_{\pm} \sum_{i=1}^3 \sum_{\mu=-1/2}^{1/2} \frac{|\langle 2S_{1/2}(m=\frac{1}{2}) | x^i | 2P_{1/2}(m=\mu) \rangle|^2}{E(2P_{1/2}) - E(2S) \pm h\nu} \\
&+ \frac{1}{3} \sum_{\pm} \sum_{i=1}^3 \sum_{\mu=-3/2}^{3/2} \frac{|\langle 2S_{1/2}(m=\frac{1}{2}) | x^i | 2P_{3/2}(m=\mu) \rangle|^2}{E(2P_{3/2}) - E(2S) \pm h\nu} \\
&\approx -\frac{1}{\nu^2} \frac{3E_{\text{fs}}}{\pi^2 (Z\alpha)^2 m_e^2 c^2} + \frac{1}{\nu^2} \frac{3E_{\text{L}}}{2\pi^2 (Z\alpha)^2 m_e^2 c^2}.
\end{aligned} \tag{13}$$

Using (3), we can integrate integrate over the black-body spectrum and obtain

$$\begin{aligned}
\Delta E''_{\text{bb}}(2S) &= \frac{\pi\alpha^3 k_B^2}{8m_e c^2} T^2 Z^2 - \frac{\alpha^4 k_B^2}{4m_e c^2} \left\{ \frac{4}{3} \ln [(Z\alpha)^{-2}] \right. \\
&+ \left. \frac{4}{3} (\ln k_0(2P) - \ln k_0(2S)) + \frac{91}{90} \right\} T^2 Z^2.
\end{aligned} \tag{14}$$

The approximation then is

$$\Delta E_{\text{bb}}(2S) \approx \Delta E'_{\text{bb}}(2S) + \Delta E''_{\text{bb}}(2S). \tag{15}$$

From Table II we see that the approximation holds for all cases studied except for the shift of the $2S$ state for ionized helium ($Z = 2$) at 4 K. The inequality (9) is not fulfilled in this case, because $\nu_{\text{max}} = 2.5 \times 10^{11}$ Hz at 4 K whereas $E_{\text{fs}}/h = 1.8 \times 10^{11}$ Hz for $Z = 2$ (see also Fig. 1). For $Z = 1$, at the same temperature, the inequality $E_{\text{fs}} \ll h\nu_{\text{max}}$ is better fulfilled, and this affords an explanation for the fact that the approximation works well in the latter case.

One would naively assume that the black-body shifts should decrease with the nuclear charge, because of the Z^{-4} scaling of the polarizability. However, that is not

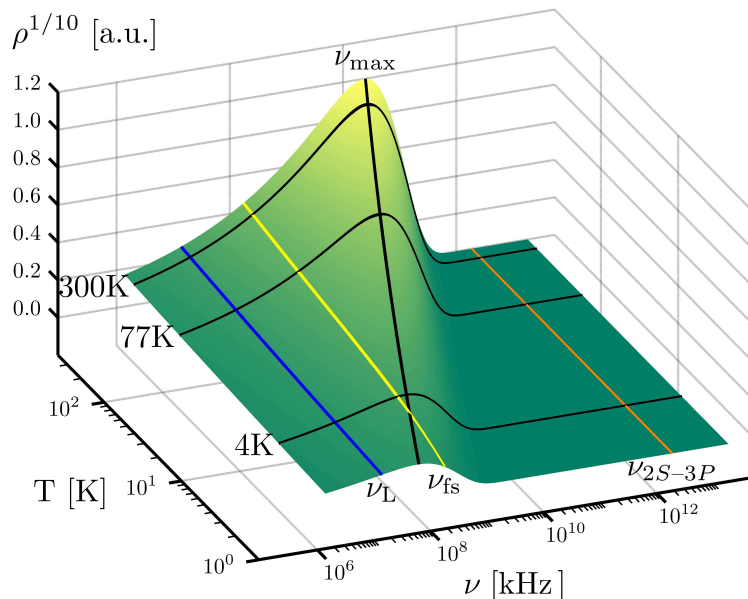


FIG. 1: The black-body spectrum given by (2) is displayed as a function of the frequency ν and of the temperature T . In order to visualize the spectrum over a wide range of temperatures, we plot $\rho^{1/10}$, and we use arbitrary units (a.u.), normalized so that ρ assumes a value of unity at its maximum (as a function of ν) for $T = 400$ K. The maximum of the blackbody spectrum as a function of the frequency at given temperature is denoted as ν_{\max} [see also Eq. (5)]. The relation of ν_{\max} to the relevant atomic frequencies, as immediately discernible from the plot, illustrates why the approximation (11) and (14) is not applicable to ionized helium at $T = 4$ K. The frequency ν_{2S-3P} is the frequency for excitation of the $2S$ state to the $3P$ state for ionized helium.

the case. The formulas (11) and (14) indicate that there are two competing effects for the shift of the $2S$ state, one which is related to virtual transitions with a change in the principal quantum number [see Eq. (11)], and another one which is related to fine-structure and Lamb shift transitions [see Eq. (14)]. The former scales with $T^4 Z^{-4}$, as expected, but the latter scales as $T^2 Z^2$, and increases with the nuclear charge number (somewhat counterintuitively). We would thus like to refer to this as an anomalous scaling. This particular behavior, in connection with planned experiments [21], has been a major motivation for carrying out the calculation report here.

Incidentally, we note that the black-body shifts at $T = 300$ K are by several orders of magnitude larger than other non-standard, non-resonant effects (“accuracy limits”) for two-photon spectroscopy recently discussed in Refs. [22, 23]. Note that after leaving the cooled nozzle in the current hydrogen atomic beam experiment [15, 16], the slow hydrogen atoms enter a high vacuum which is kept at room temperature.

III. IMAGINARY PART OF BLACK-BODY INDUCED ENERGY SHIFT

In order to evaluate the black-body induced decay rates, we have to be more precise than in Eqs. (4a) and (4b). Namely, we have to collect all the poles from the bound-state spectrum as well as integrate over the transi-

tions to the continuous spectrum, and introduce infinitesimal imaginary displacement into propagator denominators. The relevant formulas are

$$\begin{aligned}
 P_\nu(nS) &= \frac{1}{3} \sum_{i=1}^3 \left(\left\langle nS \left| x^i \frac{1}{H - i\epsilon - E(nS) - h\nu} x^i \right| nS \right\rangle \right. \\
 &\quad \left. + \left\langle nS \left| x^i \frac{1}{H - i\epsilon - E(nS) + h\nu} x^i \right| nS \right\rangle \right), \quad (16a)
 \end{aligned}$$

$$\begin{aligned}
 \Delta\mathcal{E}_{\text{bb}}(nS) &= - \lim_{\epsilon \rightarrow 0^+} \frac{e^2}{2} \int_0^\infty d\nu \bar{e}^2(\nu) P_\nu(nS) \\
 &= \Delta E_{\text{bb}}(nS) - i \frac{\Delta\Gamma_{\text{bb}}(nS)}{2}. \quad (16b)
 \end{aligned}$$

The first term on the right-hand side of (16a) describes a process with an absorption of a photon by the atom from a black-body mode, which lowers the energy of the black-body photon field in the virtual state (term $-h\nu$), and a subsequent emission into a black-body mode. For this term, the imaginary part is generated for virtual atomic states, as contained in the spectral decomposition of H , which have an energy higher than that of the reference state $E(nS)$. This is the only relevant process to generate a black-body induced width if the ground state acts as a reference state, and it is easy to see that the imaginary part of the energy shift thus generated has the cor-

TABLE II: Black-body energy shift of the $2S$ excited state of atomic hydrogen and ionized atomic helium, evaluated according to Eq. (8), expressed in terms of frequencies via division by the Planck constant h . Note that the entries for $\Delta E'_{\text{bb}}(2S) + \Delta E''_{\text{bb}}(2S)$ are given here only as an indication of the quality of the approximation given in Eqs. (11) and (14) and therefore in brackets. The entries for $\Delta E_{\text{bb}}(2S)$ are obtained by numerical integration of (4b) and thus relevant for comparison to experiment. The explanation for the discrepancy of the approximation and the numerical integration for 4 K and $Z = 2$ is given in the text (see also Fig. 1).

Nucl. charge number	Temperature	$h^{-1}\Delta E_{\text{bb}}(2S)$	$h^{-1}[\Delta E'_{\text{bb}}(2S) + \Delta E''_{\text{bb}}(2S)]$
$Z = 1$	4 K	7.79×10^{-7} Hz	$(8.13 \times 10^{-7}$ Hz)
$Z = 1$	77 K	-1.44×10^{-3} Hz	$(-1.46 \times 10^{-3}$ Hz)
$Z = 1$	300 K	-9.89×10^{-1} Hz	$(-9.87 \times 10^{-1}$ Hz)
$Z = 2$	4 K	3.40×10^{-6} Hz	$(3.30 \times 10^{-5}$ Hz)
$Z = 2$	77 K	1.18×10^{-2} Hz	$(1.19 \times 10^{-2}$ Hz)
$Z = 2$	300 K	1.21×10^{-1} Hz	$(1.21 \times 10^{-1}$ Hz)

TABLE III: Black-body induced width $\Delta\Gamma_{\text{bb}}(1S)/h$ of the ground state and of the $2S$ excited state, evaluated according to Eq. (16b) for atomic hydrogen. The results are given in Hz (cycles per second).

State	Temperature	$h^{-1}\Delta\Gamma_{\text{bb}}(nS)$
1S	300 K	1.13×10^{-163} Hz
1S	3000 K	2.15×10^{-9} Hz
1S	30000 K	8.00×10^6 Hz
2S	300 K	3.08×10^{-3} Hz
2S	3000 K	7.49×10^3 Hz
2S	30000 K	2.34×10^7 Hz

rect sign, i.e. it contributes a negative imaginary part to $\Delta\mathcal{E}_{\text{bb}}(nS)$.

The second term on the right-hand side of (16a) describes a process with (first) emission into a black-body mode, then absorption from the black-body field. In this case, the imaginary part is generated for virtual atomic states of an energy lower than that of the reference state $E(nS)$. This process can be relevant for the generation of a black-body induced decay when the $2S$ states acts as a reference state, and the virtual state is a $2P_{1/2}$ state. It is again easy to see that the imaginary part of the energy shift thus generated has the correct sign, i.e. it also contributes a negative imaginary part to $\Delta\mathcal{E}_{\text{bb}}(nS)$.

We can then easily obtain the black-body induced decay rates of the $1S$ and $2S$ states. Numerical results are given in Table III, where we restrict ourselves to atomic hydrogen. There is a very strong increase of the rates with temperature, and we note a comparatively large induced decay rate for the $2S$ state, due to the proximity of the $2P_{1/2}$ and $2P_{3/2}$ levels.

IV. CONCLUSIONS

In this paper, we have set up a formalism for the treatment of black-body induced energy shifts and corresponding decay rates (widths) for low-lying atomic states in atomic systems with a low nuclear charge. We have evaluated our expressions for the $1S$ and $2S$ states of atomic hydrogen and hydrogenlike (ionized) helium. The formula (8) leads to a consistent treatment of the virtual nP_j states ($j = 3/2$ and $j = 1/2$) which are displaced from the reference $nS_{1/2}$ state only by a fine-structure splitting and by the Lamb shift, respectively (see Sec. II), and can be easily generalized to other cases of interest. We note that all black-body shifts given in Tables I and II are well below 1 Hz in absolute magnitude and do not have to be taken into account at current and projected levels of accuracy for high-precision laser spectroscopy, although it is perhaps useful to remark that they are larger than other non-standard effects (“accuracy limits”) for two-photon spectroscopy recently discussed in the literature (Refs. [22, 23]).

The imaginary part of the black-body induced energy shift (“black-body ac Stark shift”) has been discussed and evaluated in Sec. III. The corresponding decay rates given in Table III can be quite substantial, especially at elevated temperatures. At $T = 3000$ K, the $2S$ state of hydrogen acquires a black-body width of about 8 kHz, and at $T = 30000$ K, the ground-state of atomic hydrogen is roughly 8 MHz wide, purely due to the black-body induced interactions. At the same temperature, the Boltzmann factor $\exp[-(E_{2P} - E_{1S})/(k_B T)]$ for the excitation of the ground state into the $2P$ state is only 2%.

Although the black-body energy shifts have been studied quite intensively, the numerical results and approximations have not yet appeared in the literature to the best of our knowledge. We have worked in SI units throughout this article in order to enhance the clarity of the details of the derivation.

V. ACKNOWLEDGMENTS

U.D.J. acknowledges support by the Deutsche Forschungsgemeinschaft (contract Je285/3-1).

-
- [1] T. F. Gallagher and W. E. Cooke, *Phys. Rev. Lett.* **42**, 835 (1979).
 - [2] J. W. Farley and W. H. Wing, *Phys. Rev. A* **23**, 2397 (1981).
 - [3] T. F. Gallagher, *Rydberg Atoms* (Cambridge University Press, Cambridge, 1994).
 - [4] W. M. Itano, L. L. Lewis, and D. J. Wineland, *J. Physique (Paris) Suppl.* **C8**, 283 (1981).
 - [5] W. M. Itano, L. L. Lewis, and D. J. Wineland, *Phys. Rev. A* **25**, 1233(R) (1982).
 - [6] L. Hollberg and J. L. Hall, *Phys. Rev. Lett.* **53**, 230 (1984).
 - [7] J. Varnier and C. Audoin, *The Quantum Physics of Atomic Frequency Standards* (Hilger, Bristol, 1989).
 - [8] J. J. Sakurai, *Modern Quantum Mechanics* (Addison-Wesley, Reading, MA, 1994).
 - [9] M. Haas, U. D. Jentschura, and C. H. Keitel, *Am. J. Phys.* **74**, 77 (2006).
 - [10] M. Haas, U. D. Jentschura, C. H. Keitel, N. Kolachevsky, M. Herrmann, P. Fendel, M. Fischer, T. Udem, R. Holzwarth, T. W. Hänsch, M. O. Scully, and G. S. Agarwal, *Phys. Rev. A* **73**, 052501 (2006).
 - [11] M. A. Escobedo and J. Soto, e-print 0804.0691 [hep-ph].
 - [12] M. Gell-Mann and F. Low, *Phys. Rev.* **84**, 350 (1951).
 - [13] J. Sucher, *Phys. Rev.* **107**, 1448 (1957).
 - [14] P. J. Mohr, G. Plunien, and G. Soff, *Phys. Rep.* **293**, 227 (1998).
 - [15] M. Niering, R. Holzwarth, J. Reichert, P. Pokasov, Th. Udem, M. Weitz, T. W. Hänsch, P. Lemonde, G. Santarelli, M. Abgrall, P. Laurent, C. Salomon, and A. Clairon, *Phys. Rev. Lett.* **84**, 5496 (2000).
 - [16] M. Fischer, N. Kolachevsky, M. Zimmermann, R. Holzwarth, T. Udem, T. W. Hänsch, M. Abgrall, J. Grünert, I. Maksimovic, S. Bize, H. Marion, F. P. Dos Santos, P. Lemonde, G. Santarelli, P. Laurent, A. Clairon, C. Salomon, M. Haas, U. D. Jentschura, and C. H. Keitel, *Phys. Rev. Lett.* **92**, 230802 (2004).
 - [17] M. Gavrila and A. Costescu, *Phys. Rev. A* **2**, 1752 (1970).
 - [18] K. Pachucki, *Ann. Phys. (N.Y.)* **226**, 1 (1993).
 - [19] V. Yakhontov, *Phys. Rev. Lett.* **91**, 093001 (2003).
 - [20] M. E. Rose, *Relativistic Electron Theory* (J. Wiley & Sons, New York, NY, 1961).
 - [21] M. Herrmann, M. Haas, U. D. Jentschura, F. Kottmann, D. Leibfried, S. Knünz, N. Kolachevsky, H. A. Schüssler, T. W. Hänsch, and T. Udem, submitted (2008).
 - [22] U. D. Jentschura and P. J. Mohr, *Can. J. Phys.* **80**, 633 (2002).
 - [23] L. Labzowsky, G. Schedrin, D. Solov'yev, and G. Plunien, *Phys. Rev. Lett.* **98**, 203003 (2007).